

ENVIRONMENT CANADA'S EXPERIMENTAL NUMERICAL WEATHER PREDICTION SYSTEMS FOR THE VANCOUVER 2010 WINTER OLYMPIC AND PARALYMPIC GAMES

BY J. MAILHOT, S. BÉLAIR, M. CHARRON, C. DOYLE, P. JOE, M. ABRAHAMOWICZ, N. B. BERNIER,
B. DENIS, A. ERFANI, R. FRENETTE, A. GIGUÈRE, G. A. ISAAC, N. MCLENNAN,
R. McTAGGART-COWAN, J. MILBRANDT, AND L. TONG

To provide the best possible guidance to the Olympic Forecast Team, Environment Canada has developed several experimental numerical weather prediction systems for the Vancouver 2010 Games.

On 2 July 2003, the International Olympic Committee (IOC) awarded Canada with the rights to host the 2010 Winter Games. The XXI Olympic and X Paralympic Winter Games took place from 12 to 28 February and from 12 to 21 March 2010, respectively, in the Vancouver, British Columbia, and Whistler, British Columbia, areas. The 2010 Winter Games showcased the highest-level competition at five indoor and four outdoor venues. Indoor venues include ice hockey, short-track and speed skating, figure skating, and curling, and were concentrated in the metropolitan Vancouver area. Outdoor venues were north of Vancouver (see Table 1 and Figs. 1 and 2 for locations) and included Whistler Mountain (alpine skiing), Blackcomb Sliding Centre (bobsleigh, luge, and skeleton), Callaghan Valley Olympic Park (cross-country skiing, ski jumping, biathlon, and nordic combined), and Cypress Bowl Mountain (freestyle skiing and snowboard events). Over 80 countries participated, bringing 5,500 athletes and officials to the 2010 Games. Two weeks later, ►

Photograph taken from Whistler Mountain looking northwest in the afternoon; a low-level cloud blankets Whistler Creekside ("Harvey's cloud"), and a higher deck of cloud obscures the mountain tops.

classroom training, several mountain weather workshops, and laboratories, as well as on-site venue practicum periods. The OFT, formed of 35 highly trained meteorologists from all regions of Canada and several forecasters from the U.S. National Weather Service offices in adjacent Washington State and Alaska,

provided dedicated venue forecasts during the games. An enhanced observing and monitoring network was also set up for the Olympics (details are given in the appendix). In addition to its current operational products, and in order to provide the best possible guidance and support to the OFT, Environment Canada

TABLE 1. List of the main Olympic measurement sites (already existing and new OAN sites) with their identifiers, locations (latitude–longitude), and elevations.

Main Olympic measurement sites	Identifier	Latitude (°N)	Longitude (°W)	Elevation (m)
Blackcomb Base Sliding Center Top	VOI	50°06'09"	122°56'11"	937
Blackcomb Base Sliding Center Bottom	VON	50°06'22"	122°56'32"	817
Blackcomb Mountain Base/Nesters	VOC	50°08'00"	122°57'00"	659
Callaghan Valley/Callaghan	VOD	50°08'39"	123°06'33"	884
Callaghan Valley 1 (ski jump top)	VOW	50°08'25"	123°06'15"	936
Callaghan Valley 2 (ski jump bottom)	VOX	50°08'25"	123°06'25"	860
Callaghan Valley 3 (biathlon)	VOY	50°08'51"	123°06'57"	856
Cypress bowl Event (freestyle)	VOZ	49°23'33"	123°12'07"	958
Cypress Bowl North/Cypress	VOE	49°24'07"	123°12'27"	953
Cypress Bowl South/Cypress wind	VOG	49°22'43"	123°11'39"	960
Mount Washington	VOJ	49°44'48"	125°17'13"	1474
North Cowichan	VOO	48°49'27"	123°43'06"	60
Pemberton Airport	WGP	50°18'09"	122°44'16"	204
Pemberton Airport (wind)	WPN	50°18'08"	122°44'17"	203
Pitt Meadows	WMM	49°12'00"	122°40'48"	5
Point Atkinson	WSB	49°20'00"	123°16'00"	35
Port Mellon	VOM	49°31'12"	123°28'48"	127
Powell River Airport	VOP	49°50'03"	124°30'01"	125
Qualicum Airport	VOQ	49°20'14"	124°23'38"	65
Sechelt Airport	VOU	49°27'38"	123°43'07"	86
Squamish Airport 1	WSK	49°46'54"	123°09'43"	52
Squamish Airport 2: wind profiler	XSK	49°46'54"	123°09'43"	52
Timing Flats	VOT	50°05'30"	122°58'49"	797
Vancouver International Airport	YVR	49°12'00"	123°10'00"	4
West Vancouver	WWA	49°20'50"	123°11'31"	168
Whistler Mountain High Level/Pig Alley	VOA	50°04'37"	122°56'51"	1640
Whistler Mountain High Level/remote wind	VOH	50°04'27"	122°56'49"	1643
Whistler Mountain Low Level/Creekside	VOB	50°05'17"	122°58'32"	933
Whistler Mountain Mid-Station	VOL	50°05'07"	122°57'51"	1320
Whistler CWO Snowfall Verification System	WAE	50°08'00"	122°57'00"	659
White Rock	WWK	49°01'00"	122°46'00"	13
Non-Environment Canada sites				
MOC Roof Auto 8 and RVAS	MOC	49°10'58"	123°04'43"	20
Roundhouse	RND	50°04'45"	122° 56.818°	1856
Whistler Peak	AQRB	50°03'55"	122° 57.485°	2165

has developed the following experimental numerical weather prediction (NWP) systems for the Vancouver 2010 Games: 1) a regional ensemble prediction system (REPS), 2) a high-resolution deterministic prediction system, and 3) an external land surface modeling system at the microscales.

This paper focuses on a description of these experimental numerical prediction systems, together with some examples and verification results from the winters of 2008 and 2009 using the enhanced Olympic observing network.

NWP SUPPORT TO THE WINTER GAMES.

NWP in previous winter games. The Olympic Games have often been an opportunity to develop and test new, advanced forecasting systems. For the 2002 Winter Games in Salt Lake City, Utah, an Olympic weather support system was developed by government agencies, private firms, and the University of Utah (Onton et al. 2001; Horel et al. 2002). Apart from the installation of several cooperative observing mesonetworks, and their later integration into MesoWest and SnowNet, real-time mesoscale numerical modeling was done using the fifth-generation Pennsylvania State University (PSU)–National Center for Atmospheric Research (NCAR) Mesoscale Model (MM5) with three nested grids of 36-, 12-, and 4-km

horizontal grid spacings, incorporating MesoWest observations into the near-surface initial conditions. This Olympic system was found to often outperform the operational models over complex terrain, mostly because of its better resolution of orographic features.

For the 2006 Winter Games in Torino, Italy, the ARPA Piemonte Italian Weather Service developed an advanced system combining a very dense weather-observing network, high-resolution numerical modeling, and a distributed weather office network with well-trained forecasters (Oberto et al. 2007). New techniques and procedures were developed for the Torino Olympics, which led to a significant legacy for Alpine weather forecasting. Stauffer et al. (2007) showed that the accuracy of MM5 forecasts for the Torino 2006 Olympics increased, especially near the surface and in the boundary layer, with higher model resolution (using an additional nested grid at 1.3 km) and with data assimilation of the special observing network.

NWP support to the Vancouver Games. Because of their proximity to the coastal waters of the Pacific Ocean and the surrounding complex terrain, most Vancouver Olympic venues can experience a wide range of rapidly changing winter weather conditions that pose great challenges for the forecasters. During the month of February alone, for instance, typical precipitation amounts vary from less than 130 mm in the rain shadow of Vancouver Island to more than 400 mm on the coastal mountains. Stretching out from Vancouver to Whistler over a distance of about 120 km, and serving as the main ground transportation corridor, the Sea-to-Sky Highway rises from sea level to an altitude of 660 m. The top of the downhill ski runs are about 1000 m higher. While it can be overcast and rainy in Vancouver and Cypress Mountain, conditions at Callaghan Valley and Whistler–Blackcomb can be a mix of rain and snow, with low visibility resulting from fog and low ceilings, and strong gusty winds at the mountaintops. Local effects can be particularly important, with wind channeling and drainage flow in the narrow mountain valleys, terrain-induced upslope flows leading to fog and low cloud formation, such as Harvey’s Cloud at Whistler mid-mountain (Fig. 3), and heavy snowfall and rapid changes in precipitation types.

In addition to focusing more attention on the various forecasting challenges at the Olympic venues, the experimental NWP systems developed for the Vancouver 2010 Winter Games were tailored to fit several specific needs and requirements of the

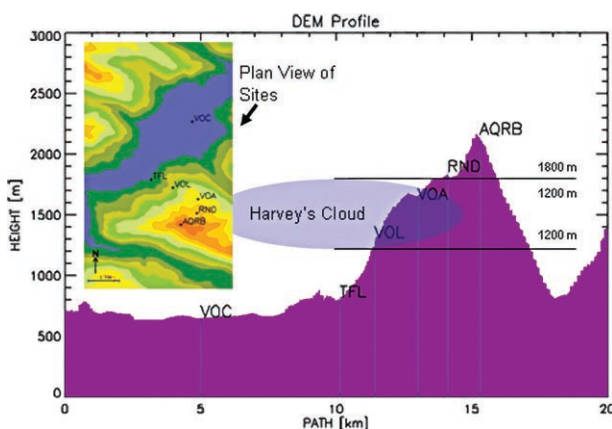


FIG 3. A profile of Whistler Mountain, the site of the downhill, slalom, and super G alpine events, showing the elevation of various observation sites such as Nesters (VOC), Timing Flats (TFL), Mid-Station (VOL), Pig Alley (VOA), Roundhouse (RND) and Whistler Peak (AQRB). Harvey’s Cloud, a persistent cloud on the mountain, is marked in blue and constitutes a major potential risk of reduced visibility for skiers, right in the middle of the downhill ski course. The cloud is fondly named after Harvey Fellowes, a long-time employee of the Whistler-Blackcomb ski resort, who spent quite a few years on the hill and noted the looming and frequent presence of this cloud on the ski hill.

TABLE 2. The threshold matrix for the Alpine events (downhill, slalom, and giant slalom), showing the specific criterion used for decision factors by the competition judges with respect to various meteorological conditions. Similar matrices exist for the other Olympic sport events.

Threshold matrix for downhill, slalom, and giant slalom events					
	New snow (24 h)	Wind	Visibility	Rain	Wind chill
Critical decision point	> 30 cm	Constant above 17 m s ⁻¹ or gusts > 17 m s ⁻¹	< 20 m on entire course	15 mm in 6 h or less	< -25°C
Significant decision point	> 15 cm and < 30 cm	Constant 11–17 m s ⁻¹	20 m on portions of the course	Mixed precipitation	
Factor to consider	<ul style="list-style-type: none"> • 5 cm • 2 cm, within 2 h of the event 	Gusts above 14 m s ⁻¹ but < 17 m s ⁻¹	> 20 m but < 50 m on all or part of the course		

users. Some Olympic competitions have extremely sensitive thresholds for their decision process. For instance, the Alpine events, such as the downhill, giant slalom, and slalom held at Whistler (Table 2), rely on specific thresholds for a go/no-go decision. Weather elements that are considered include new snow or rain amounts over the last 6–24 h, winds and wind gusts, visibility on all or portions of the ski course, and wind chill factor. Accurate information on such parameters influences critical and significant decision points or represents factors of consideration by the event judges.

The design and configuration of the experimental NWP systems also took into account several strategic constraints. These include the timely delivery of model output products twice a day, complying with the schedules of weather briefings of the Olympic Forecast Team, which mainly focuses on the period after the 6-h forecasts. Routinely, a morning briefing is held between 0700 and 0800 LT to provide enhanced weather forecast guidance for the sport competitions of the day. An early afternoon briefing (1300–1400 LT) provides updated forecasts to support competitions held in the evening (e.g., some nordic and freestyle skiing events) and gives an outlook at the weather for the early morning of the next day.

REGIONAL ENSEMBLE PREDICTION SYSTEM. In collaboration with McGill University (Montréal, Quebec, Canada), a REPS has been developed for probabilistic short-range weather forecasting. It is based on the limited-area version of the Global Environmental Multiscale Model (GEM-LAM), with 20 members at 33-km horizontal grid spacing covering the North American continent and adjacent oceans. The REPS is dependent on the Canadian Meteorological Centre (CMC) operational

global ensemble prediction system (EPS); each of its 20 members are initialized and laterally driven by a global EPS member (100-km horizontal grid spacing). Note that the global EPS is based on an ensemble Kalman filter assimilation system, including a representation of model errors and using four-dimensional handling of observations that are valid at different times in the data assimilation window (Houtekamer et al. 2007, 2009). The model’s subgrid-scale parameterizations for the REPS are identical to the deterministic GEM described in Bélair et al. (2009). Stochastic perturbations are applied to the subgrid-scale physical tendencies of horizontal winds and temperature. An example of probabilistic precipitation forecast with the REPS is shown in Fig. 4, and other examples of REPS outputs will be shown in a subsequent section.

The Canadian REPS was one of the participating systems in a Research Development Project (RDP) endorsed by the World Weather Research Programme (WWRP) of the World Meteorological Organization (WMO) focusing on mesoscale ensemble forecasting for the 2008 Beijing, China, Summer Olympics. During this period, a version of the REPS with 20 members at 15-km horizontal grid spacing was run daily.

In the context of preparing dedicated weather forecast systems for the Vancouver 2010 Winter Olympics, the 33-km version of the REPS was first available to the OFT for evaluation and training during February 2008 and February 2009, and essentially the same system was also available during the 2010 games. After performing objective verification in winter with a variety of probabilistic measures, it has been decided that an REPS on a smaller domain with 15-km grid length did not add value to the 33-km version. The latter version has thus been selected.

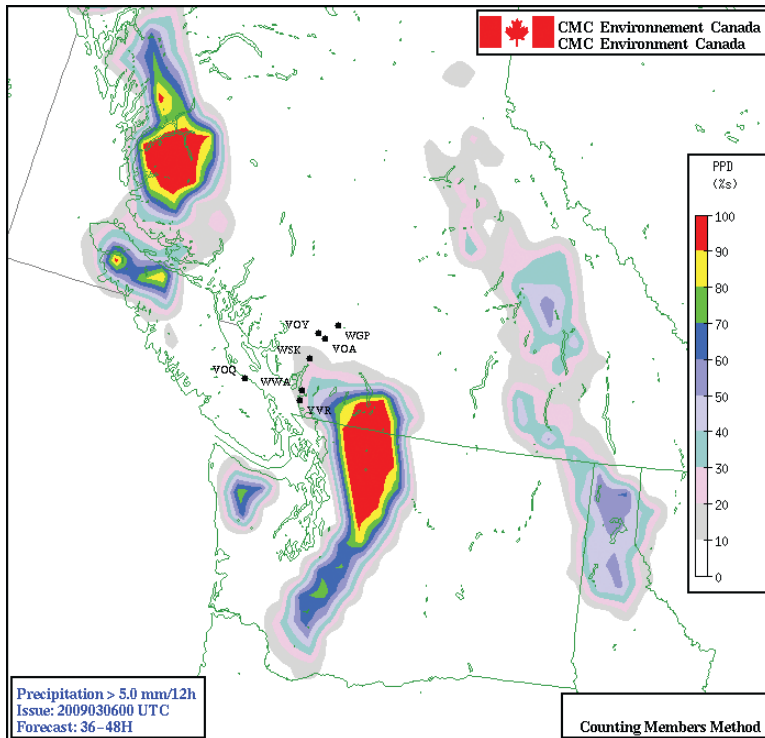


FIG 4. Example of probabilistic precipitation forecast with the 33-km REPS. The probability that the accumulated precipitation (equivalent liquid water) will be greater than 5 mm during the 12-h time interval (forecast lead time from 36 to 48 hours) from 1200 UTC 7 March to 0000 UTC 8 March 2009 is shown on the color bar. The Vancouver (YVR), West Vancouver (WWA), and Squamish (WSK) areas lie in the regions of 10%–30% of probability of precipitation (in pink) while Callaghan Valley (VOY), Whistler (VOA), and Pemberton (WGP) have probability of precipitation less than 10%.

MESOSCALE DETERMINISTIC PREDICTION SYSTEM.

The second component of the experimental numerical prediction systems used for the Vancouver games is a high-resolution NWP model with improved geophysical fields and cloud microphysics and radiation schemes, and with new diagnostic model outputs. This mesoscale prediction system consists of three one-way-nested GEM-LAM grids (at 15-, 2.5-, and 1-km grid spacings; see Fig. 5) integrated for 19 h, twice a day, from the 0000 and 1200 UTC regional 15-km GEM operational runs (Mailhot et al.

2006). Note that data assimilation is only used in the regional 15-km GEM runs. (Currently, no special mesoscale data assimilation system is available for the high-resolution GEM-LAM grids.) The configuration of the high-resolution modeling prototype is schematized in Fig. 6. The 15- and 2.5-km grids of the Olympics system are essentially clones of the GEM-LAM system currently operational at CMC (Erfani et al. 2005), with the main differences being that they are integrated over a smaller domain and for a shorter period, and that they use several improvements to the physics package, as follows:

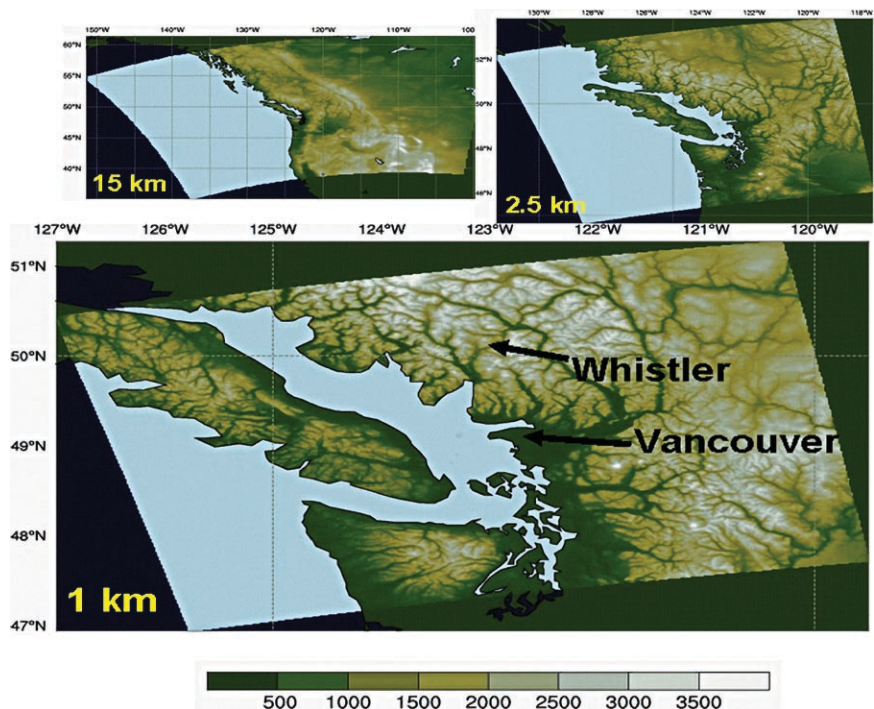


FIG 5. The domains of the high-resolution forecast prototype for the Olympics consisting of a cascade of three one-way nested grids with 15-km, 2.5-km, and 1-km horizontal grid-spacings covering the Vancouver and Whistler areas. The shading indicates the terrain elevation (in m according to scale at bottom of figure).

- Geophysical fields: Improved orography, land–sea mask, and surface roughness length fields have been generated from a recent geophysical database at high resolution (90 m) using newly developed geophysical processor software.
 - Cloud microphysics scheme: The prototype uses the double-version of the Milbrandt–Yau microphysics scheme (Milbrandt and Yau 2005) where two moments of the particle size distribution, proportional to the mass mixing ratio and total number concentration, respectively, of each of the six hydrometeor categories are independently predicted. The double-moment approach leads to more accurate calculations of the microphysical growth/decay rates (source/sink terms) and sedimentation (i.e., precipitation) rates compared to single-moment schemes, which predict only one moment (generally the mixing ratio), and are more commonly used because of computational restraints. It also permits better identification of particle types, for example, the distinction between drizzle and rain (for a given liquid water content), because the size distribution spectra can evolve more freely. Several other improvements to the microphysics parameterization have been made. This includes a diagnostic bulk snow density and a new precipitation rate (volume flux) of the total unmelted “snow” (based on the combined precipitation rates of the ice, snow, and graupel categories), which allows for the prediction of an instantaneous solid-to-liquid ratio (snow-water equivalent) for solid precipitation (Milbrandt et al. 2009). To the authors’ knowledge, this is the first time a fully double-moment microphysics scheme will be used for this type of operational forecast system.
 - Radiation and cloud–radiation interactions: The radiative transfer scheme of Li and Barker (2005) has been included in the Olympic prototype, correcting the cold bias during winter conditions and providing more realistic temperature forecasts under such situations. Other components of the radiation package have also been improved, such as cloud–radiation interactions (cloud optical properties, liquid/solid partition, etc.).
- Furthermore, special emphasis was put on developing several new diagnostic outputs from the high-resolution models, such as wind gusts, visibility, precipitation types, and snow-to-liquid ratio, all presented with a customized output package, as follows:
- Wind gusts and 10-m wind variances: Near-surface wind gusts associated with surface layer turbulence and large eddies in the boundary layer are diagnosed from the turbulent variables in the model. Wind gusts [the wind gust estimate

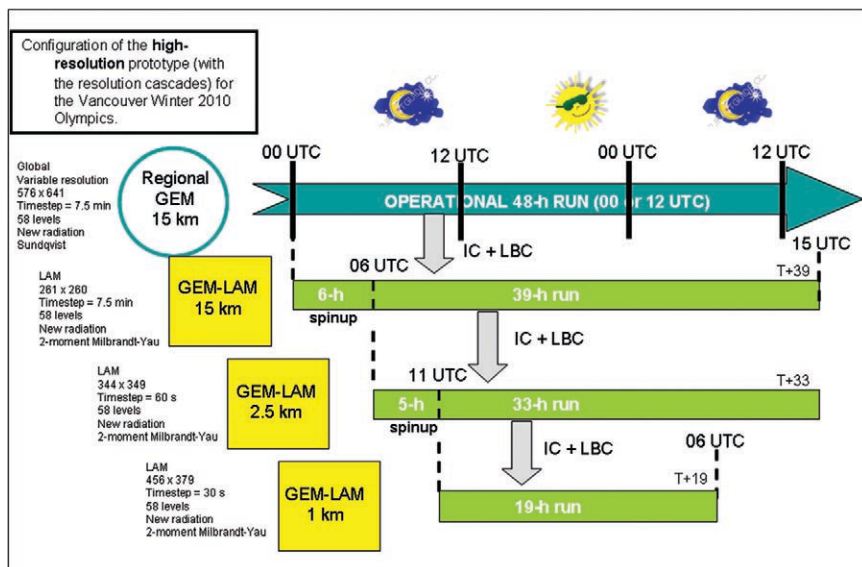


FIG 6. The daytime configuration (i.e. from 0000 UTC) of the high-resolution modeling prototype for the Vancouver 2010 Winter Olympics. The cascade of integrations goes the following way: 1) a GEM-LAM 15-km run is initialized from the 0-h forecast of the Regional GEM 15-km run started at 0000 UTC (boundary conditions for the GEM-LAM integration are also provided by the regional run) and integrated for 39 h until 1500 UTC the following day; 2) a GEM-LAM 2.5-km run is initialized at 0600 UTC from the 6-h forecast (allowing for the model spinup period) of

the GEM-LAM 15-km run started at 0000 UTC (which also provides the boundary conditions) and integrated for 33 h until 1500 UTC the next day; 3) the GEM-LAM 1-km run is then initialized at 1100 UTC from the 5-h forecast of the 2.5-km run (which also provides the boundary conditions) and integrated for 19 h until 0600 UTC the next day. The same procedure is repeated for the regional 15-km GEM run starting at 1200 UTC to provide the Olympics cascade (15, 2.5, and 1 km) forecasts valid for the afternoon and evening (from 2000 to 1500 UTC; i.e., from 1200 to 0700 LT).

together with lower and upper bounds, based on the method of Brasseur (2001)] and standard deviations of 10-m wind speed and direction are available as 2D output fields.

- Visibility: The visibilities through fog (cloud water), rain, and snow, and “total” visibility (resulting from the combined effects of the reduction of visibility from all three) are available as 3D diagnostic output variables. The computations are based on empirical relations to the cloud water content and the droplet number concentration, and the precipitation rates of drizzle/rain and snow, respectively.
- Snow-to-liquid ratio of precipitating snow: As mentioned above, the snow-to-liquid ratio of falling “snow” (ice crystals, aggregates, and graupel) is obtained as a new diagnostic output. The solid-to-liquid ratio can vary between values of around 2.5 (for very dense snow, either heavily rimed or partially melted) to values of over 30 (for very low-density snow, such as large aggregates).
- Various diagnostic levels: Several 2D fields have been added, such as the heights above ground of cloud base, freezing levels (either as the first 0°C isotherm from the ground or from above), and snow level (lowest level with a nonzero falling snow rate).
- Customized output package: Based on the feedback from the OFT after the practicum periods of winters 2008 and 2009, a list of useful products has been finalized, together with specifications related to the display format that could be easily used by the forecasters at the different Olympic venues. The comprehensive list of model outputs

includes 2D maps, time series or meteograms at a number of surface stations, cross sections along specific lines, and vertical soundings at standard and additional Olympic locations. Examples of these outputs will be presented later on.

EXTERNAL LAND SURFACE PREDICTION AND ASSIMILATION SYSTEM.

Land surface modeling is traditionally done “in line” in numerical atmospheric models, with full two-way interactions between the atmospheric and surface components of the model. In this approach, the spatial resolution of the simulations is severely limited by the large computational cost of the atmospheric component of the coupled system.

This limitation can be avoided, and significant refinement in surface and near-surface forecasts (e.g., air temperature, low-level winds, soil moisture, and snow canopy) can be achieved by running an external high-resolution surface model in a prognostic mode driven in a one-way fashion by atmospheric forcing provided either by a coarser-resolution atmospheric model or by observations. Because a surface model can run at a fraction of the cost of the atmospheric component, its spatial resolution is mainly limited by the resolution of the datasets available to define the local characteristics of the land surface (e.g., orography, vegetation, and soil characteristics). Two strategies are proposed to achieve this refinement of surface and near-surface numerical forecasts for the Vancouver 2010 Winter Games.

Two-dimensional high-resolution external land surface model. The first strategy uses the external high-

resolution (or microscale) prognostic surface model driven from 0 to 48 h by available outputs from the operational 15-km regional model (Mailhot et al. 2006) and from the 33-km global medium-range model (Bélair et al. 2009) afterward (up to 96 h). The approach is schematically illustrated in Fig. 7. For numerical predictions over natural land covers, the Interactions between Surface, Biosphere, and Atmosphere (ISBA; Noilhan and Planton 1989) land surface scheme is integrated on a 100-m grid over a 140 km × 180 km domain (1400 × 1800 points; see Fig. 8).

The best-available land surface information was compiled and used to define local land characteristics. For

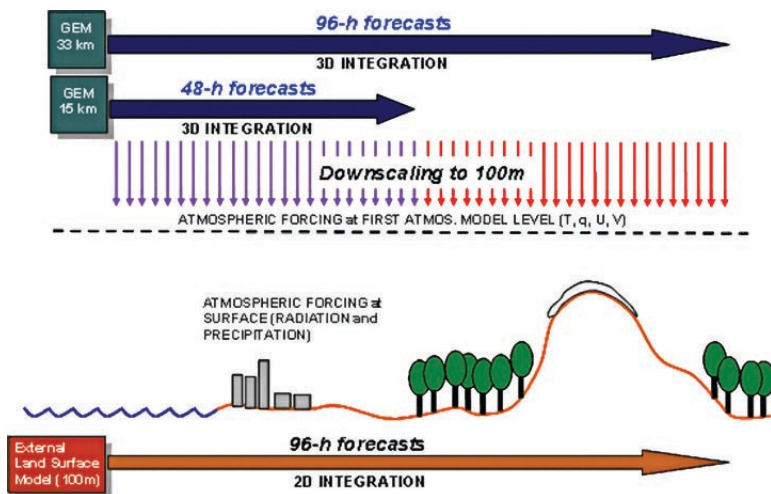


FIG 7. Schematic description of the external high-resolution surface system proposed for deterministic predictions during the Vancouver 2010 Winter Olympics.

instance, microscale topographic information was obtained from the Shuttle Radar Topography Mission Digital Elevation Model (SRTM-DEM) to specify the orography over the domain of the microscale surface model (Fig. 8). Several new databases have also been acquired for land use–land cover (LULC), such as the GlobCover global database at 300 m and several Canadian databases obtained from the Canadian Centre for Remote Sensing (CCRS) at 250 m and from the Earth Observation for Sustainable Development of Forests (EOSD) at 25 m.

The atmospheric forcing fields required to drive the external land surface system (i.e., low-level air temperature, humidity, and winds, as well as surface pressure, downwelling shortwave and longwave radiation, and precipitation) are provided by the lower-resolution regional and global atmospheric models. Some of these forcing variables are down-scaled to the high-resolution external land surface computational grid in a simple manner. Knowing the exact height difference (for each point) of orography between the high-resolution (100 m) external computational grid and the low-resolution atmospheric forcing grid, and assuming a constant lapse rate of 0.0060 K m^{-1} , it is possible to adapt or down-scale surface pressure and air temperature from the 15- or 33-km GEM forecasts using the hydrostatic approximation. This adapted air temperature is then used to downscale low-level air humidity, by assuming conservation of relative humidity, and to possibly change precipitation phase. Despite its simplicity, this adaptation process leads to a more realistic representation of the spatial variability of surface variables in complex terrain, as shown by the snow depth forecast given in Fig. 8.

As a preliminary step pending the development of a detailed land data assimilation system, initial conditions of the prognostic surface variables (e.g., snow surface temperature, snow depth, etc.) are simply obtained from the 24-h external microscale forecast of the previous day. In this simple approach, the atmospheric forcing is thus provided by the

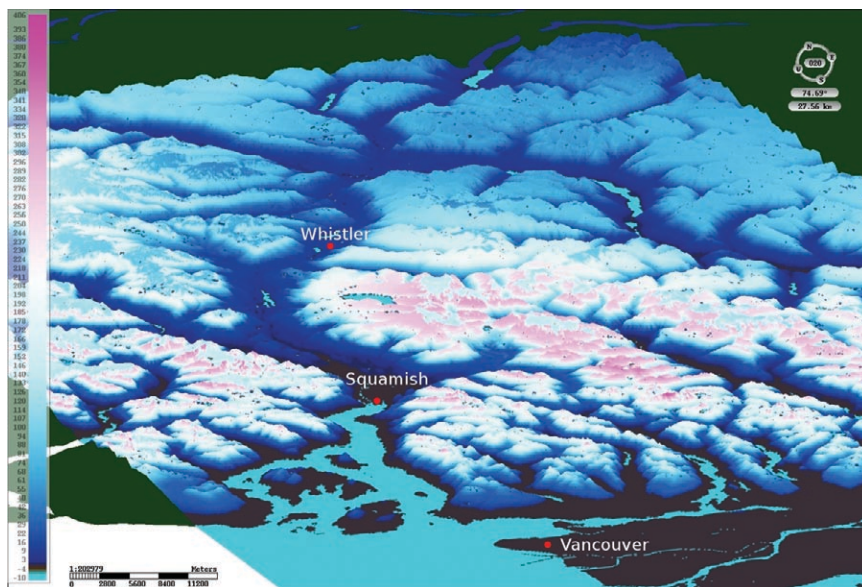


FIG 8. The domain of the 1400x1800 computational grid of the external microscale (100-m horizontal grid-spacing) surface system. The colors indicate an example of snow depth produced by the 100-m surface prediction system. Snow depth according to scale at left of figure.

adapted 15-km regional outputs without any direct assimilation of observations (in a so-called “open loop” manner).

Single-point external land surface prediction system. In this other external system, the land surface scheme ISBA land surface model is integrated at particular locations only (i.e., at a set of single-point locations corresponding to the OAN surface observing stations), for which local characteristics such as elevation, vegetation type, and vegetation fractional coverage, are well known. The single-point forecasts are also driven by downscaled atmospheric forcing from the 15-km regional model for the first 48 h and from the 33-km global model for the next 48 h.

The land surface initial conditions used in these predictions are obtained with an approach similar to the external 2D microscale system, except, however, that atmospheric forcing is provided by station observations (when available; otherwise, forcing is provided by the regional model), and snow depth observations are assimilated using a simple optimal interpolation technique. This improvement in initial conditions is clearly an advantage compared with the above 2D system, and indeed led to much improved predictions of surface and near-surface conditions (even though only at the surface observational stations). The single-point system was successfully tested during the 2008 and 2009 practicums, and an example of the products is shown in the next section.

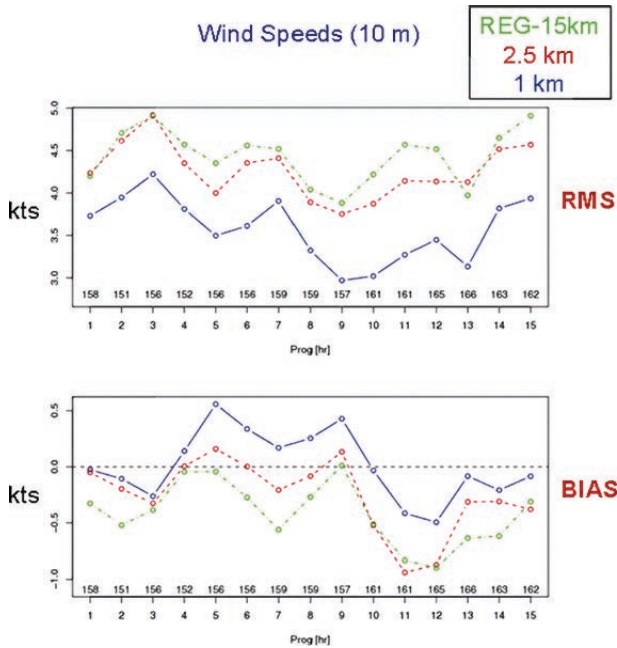


FIG 9. Time evolution (1–15-h forecasts) of objective verification scores [root-mean-square (RMS) errors and bias] against the OAN for 10 cases of winter 2008 for 10-m wind speeds (in knots). Notable improvements are found with the 1-km model (in blue) for the winds compared to the 2.5-km model (in red) and the regional 15-km model (in green).

EXAMPLES OF OLYMPIC PROTOTYPE FORECASTS AND VERIFICATIONS.

Objective verification of high-resolution models poses many challenges and must be based on high-resolution observation networks, such as surface mesonetworks and radar imagery. We took advantage of the new OAN for verification of the high-resolution Olympic prototype. Despite a relatively large number of surface stations (about 40), it is recognized that the OAN is concentrated over a rather small region covering the Olympic venues (cf. Fig. 1). Preliminary verification of the high-resolution 3D deterministic model work was based on 10 cases of significant weather from the winter of 2008, which, according to the practicum forecasters, were representative of “bad” weather conditions over the various Olympic sites. These cases included frontal passages, valley clouds, heavy snowfall, mixed-phase precipitation, and strong wind gust events. Objective verification scores against the OAN for the 10 cases indicate significant improvements with the 1-km grid for the near-surface winds (Fig. 9) compared to the 2.5-km and the regional 15-km models. For temperatures (not shown), both the 1- and the 2.5-km grid configurations show notable improvements compared to the regional 15-km model. Objective verification has continued throughout the winter 2009 practicum period, together with subjective verifications and feedback from the Olympic forecast team.

Some examples of the Olympic prototype model outputs are shown in Figs. 10–12. They are drawn mostly from the forecast experience of A. Giguère, one of the forecasters on the

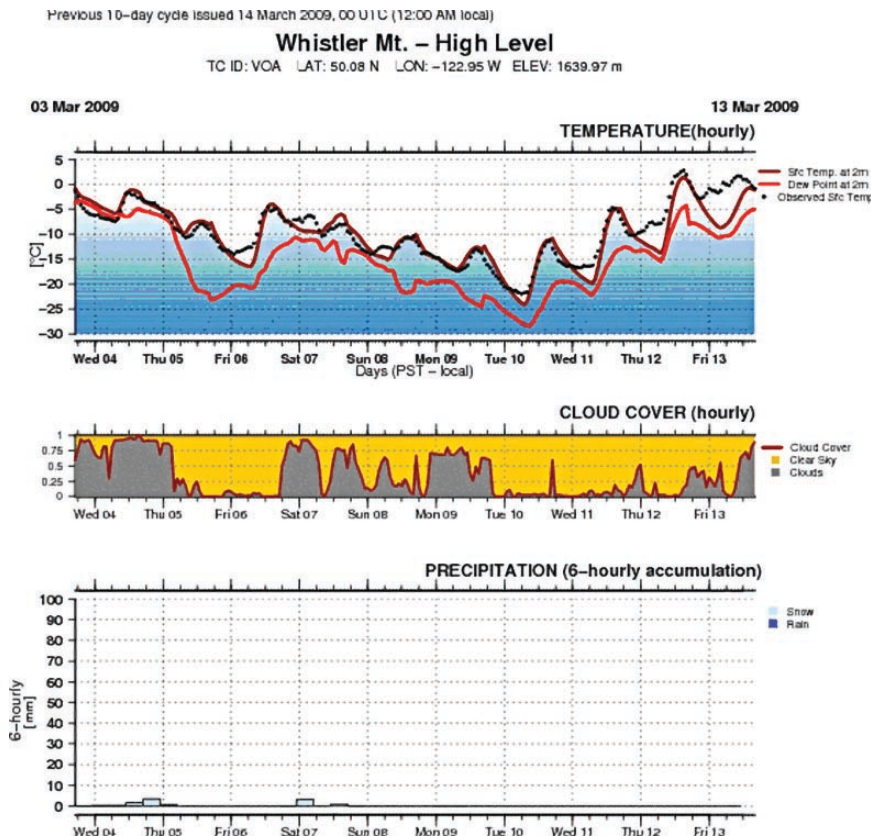


FIG 10. Point forecast of the single-point surface model at VOA (Whistler Mountain High Level–Pig Alley) for the period from 4 to 13 March 2009 for 2-m air temperature (°C), 2-m dew point temperature (°C), cloud cover, and precipitation (mm). Temperature observations appear as black dots. Note how the forecasts of temperature fit well the observations but their minima are generally too low under clear skies conditions.

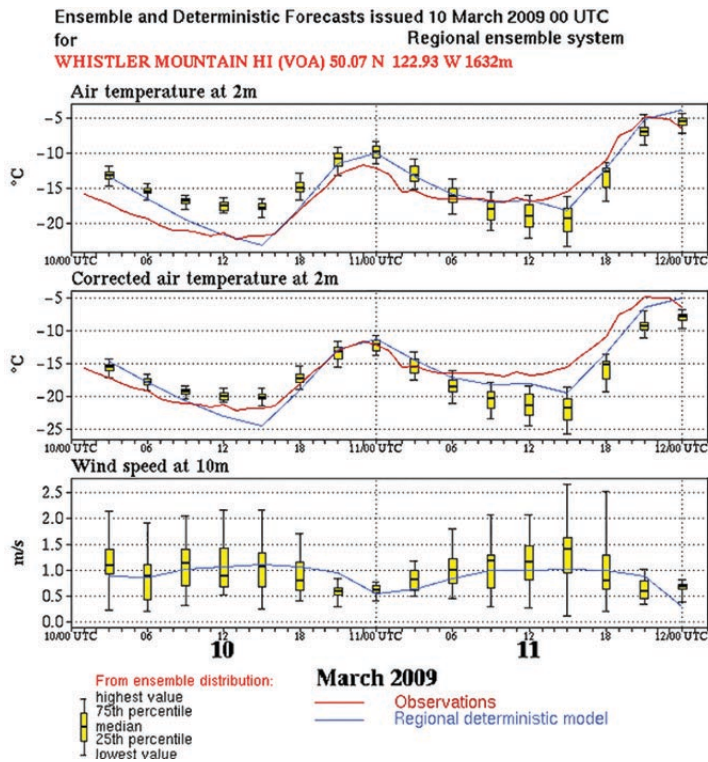
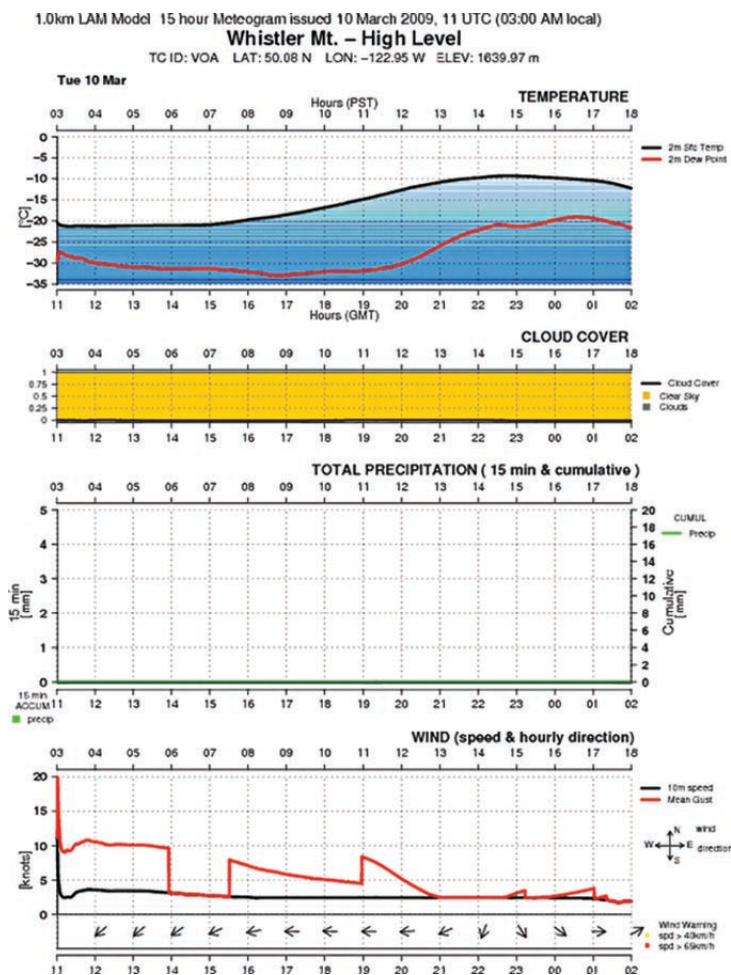


FIG 11 (LEFT). Combined meteograms of ensemble and deterministic forecasts at VOA (Whistler Mountain High Level–Pig Alley) for 10–11 March 2009. Regional Ensemble Prediction System (REPS) forecasts for 2-m air temperature, “corrected” 2-m air temperature, and 10-m wind speed (m s^{-1}). Deterministic forecasts from the Regional 15-km GEM are shown in blue and observations of air temperature are shown in red (wind observations are missing). Corrected 2-m air temperature is obtained using a dry adiabatic lapse rate between the actual altitude of the observation station and the corresponding model terrain height.

FIG 12 (BELOW). Meteograms of the Olympic GEM-LAM 1-km forecasts starting at 1100 UTC 10 March 2009 at VOA (Whistler Mountain High Level–Pig Alley) for surface temperature and dew point, cloud cover, precipitation, wind (speed and hourly direction) and estimated wind gust.

OFT, at the Alpine ski venue during the 2009 practicum period (January–March 2009), which represented the final opportunity to test the Olympic prototype in an operational setting. A forecast challenge came up on 10 March 2009 with expected very low temperatures combined with winds, so that the wind chill factor could be an issue during practice runs for a Paralympic Alpine Skiing World Cup downhill event. Models were consistent in forecasting wind chill factors of -25°C or less (not shown), which are rather infrequent in Whistler, especially in March. Two useful tools for anticipating those very low temperature minima were the meteograms of the single-point surface model (Fig. 10) and those combining the REPS forecast and the deterministic output of the GEM regional model (Fig. 11). In general, the single-point surface model gave impressive forecasts for the daytime temperature maxima and minima in agreement with observations, except under clear skies where the minima are too low. On 10 March, near-record-low dewpoint temperatures (with values of around -30°C) were also both forecasted (Figs. 10 and 12) and observed (not shown), resulting in relative humidity of less than 20%. Although models were doing well on forecasting these values (cf. Figs. 10



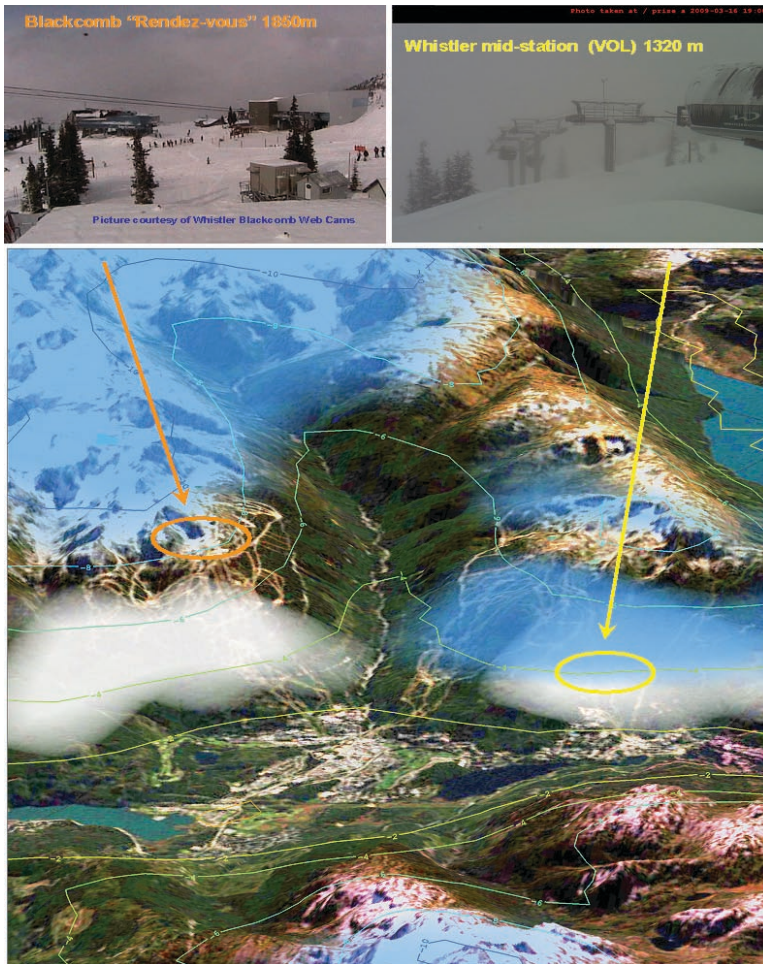


FIG 13. Pictures from the Whistler and Blackcomb web cameras at Mid-Station VOL (upper right) and “Rendez-vous” (upper left) locations taken at 1900 UTC (12:00 local time) on 16 March 2009 with the corresponding GEM-LAM 1-km forecast of isotherms of 2-m air temperature [color contours (°C)] and of clouds containing liquid droplets (white shading) and ice crystals (blue shading).

and 12), forecasters were actually reluctant to forecast dewpoints so low, and their adjusted forecast dewpoints ended up being at least 5° too high.

As already mentioned, another interesting forecast challenge is the generation of a stratocumulus (Sc) cloud deck forming in the Whistler valley flow and clinging to the mountainside, the so-called Harvey’s Cloud. This occurred, for instance, on 16 March 2009 and allowed for assessment of the height of cloud bases predicted by the LAM Olympic prototype. The pictures taken by the Whistler–Blackcomb webcams (Fig. 13) indicate that Whistler Mountain Mid-Station (VOL) was in the fog while the top of Blackcomb Mountain (“Rendez-vous”) was simply overcast by an elevated cloud layer, with a Sc cloud deck that was visible down below. The visibility sensor and snowfall-rate observations (not shown) also confirm

that it was snowing at VOL and VOA (Whistler Mountain High Level-Pig Alley; cf. Table 1 and Figs. 2 and 3) and that the precipitation was forming lower down the mountain. The corresponding forecast (Fig. 13) at 1900 UTC (1200 LT) from the GEM-LAM 1-km prototype indicates the presence of several cloud layers with low cloud bases over Whistler Valley and higher cloud bases over the mountains, with the lower-based Sc cloud deck being “pushed” up the valley.

OUTLOOK. Following the 2009 practicum period, a few adjustments to the experimental numerical prediction systems have been done to produce the final version of the Olympics high-resolution forecasting systems, which were delivered in time for the 2010 Olympic and Paralympic Games. As in previous winter games (e.g., Salt Lake City and Torino), the Vancouver 2010 games presented a unique opportunity to leave a significant legacy through science and technology with the development and testing of new EPS and high-resolution NWP systems, microscale surface adaptation models, and nowcasting systems. These advanced systems have been used daily by the forecasters of the OFT during the

games in their internal weather discussions, their forecasts, and their preparation for daily briefings with competition venue managers and team coaches, especially for weather-sensitive events such as alpine skiing, freestyle skiing aericals, and ski jumping. In the future, these systems will improve Environment Canada’s predictive capability for high-impact winter weather in complex alpine terrain through their transfer to the operational activities of the CMC and regional storm prediction centers and through the training of operational meteorologists familiar with those new tools.

ACKNOWLEDGMENTS. The development and final configuration of the experimental NWP systems greatly benefited from the continuous feedback from our colleagues from the Pacific Storm Prediction Centre (PSPC)

in Vancouver, Brad Snyder and Trevor Smith, and from the Olympic Forecaster Team (in particular, Ivan Dubé, Matt Loney, Carl Dierking, and Andrew Teakles). The collaboration of Xiaoli Li and Prof. Peter Yau of McGill University in the development of the REPS, of André Plante (CMC) for the mesoscale objective verification package, and of Jean-Philippe Gauthier (CMC) for the generation of images is warmly acknowledged. Thanks are also due to Al Wallace, director of PSPC, for providing some of the material presented in the introduction. The final version of the manuscript benefited from the constructive comments of two anonymous reviewers.

APPENDIX: A SPECIAL OBSERVING NETWORK FOR THE OLYMPICS.

Until 2007, the mountainous corridor between Vancouver and Whistler was rather data sparse; there were a few stations around Vancouver, an automated station at Squamish (about midway between Vancouver and Whistler), and a partial day-manned observing station at Whistler. An enhanced monitoring system has been set up for the Olympics, consisting of an OAN and several sites instrumented with various types of profilers (boundary layer wind profilers, microwave radiometers, ceilometers, visibility meters), a C-band weather radar and two vertically pointing X-band radars, and supplementary radiosondes. The main Olympic measurement sites are listed in Table 1. The OAN (Figs. 1 and 2) consists of about 40 standard and special surface observing sites with hourly or synoptic reports available on the Global Telecommunication System (GTS) of surface pressure, temperature, relative humidity, wind speed and direction, precipitation rate, and snow depth. The installation of the entire network was completed in the autumn of 2007, giving two complete winters of learning from the data before the 2010 Winter Games.

REFERENCES

- Bélaïr, S., M. Roch, A.-M. Leduc, P. A. Vaillancourt, S. Laroche, and J. Mailhot, 2009: Medium-range quantitative precipitation forecasts from Canada's new 33-km deterministic global operational system. *Wea. Forecasting*, **24**, 690–708.
- Brasseur, O., 2001: Development and application of a physical approach to estimating wind gusts. *Mon. Wea. Rev.*, **129**, 5–25.
- Erfani, A., J. Mailhot, S. Gravel, M. Desgagné, P. King, D. Sills, N. McLennan, and D. Jacob, 2005: The high resolution limited area version of the Global Environmental Multiscale model (GEM-LAM) and its potential operational applications. Preprints, *11th Conf. on Mesoscale Processes*, Albuquerque, NM, Amer. Meteor. Soc., 1M.4. [Available online at <http://ams.confex.com/ams/pdfpapers/97308.pdf>]
- Horel, J., T. Potter, L. Dunn, W. J. Steenburgh, M. Eubank, M. Splitt, and D. J. Onton, 2002: Weather support for the 2002 Winter Olympic and Paralympic Games. *Bull. Amer. Meteor. Soc.*, **83**, 227–240.
- Houtekamer, P. L., M. Charron, H. L. Mitchell, and G. Pellerin, 2007: Status of the global EPS at Environment Canada. *Proc. ECMWF Workshop on Ensemble Prediction*, Reading, United Kingdom, ECMWF, 57–68.
- , H. L. Mitchell, and X. Deng, 2009: Model error representation in an operational ensemble Kalman filter. *Mon. Wea. Rev.*, **137**, 2126–2143.
- Li, J., and H. W. Barker, 2005: A radiation algorithm with correlated-*k* distribution. Part I: Local thermal equilibrium. *J. Atmos. Sci.*, **62**, 286–309.
- Mailhot, J., and Coauthors, 2006: The 15-km version of the Canadian regional forecast system. *Atmos.–Ocean*, **44**, 133–149.
- Milbrandt, J. A., and M. K. Yau, 2005: A multimoment bulk microphysics parameterization. Part II: A proposed three-moment closure and scheme description. *J. Atmos. Sci.*, **62**, 3065–3081.
- , D. Jacob, and R. McTaggart-Cowan, 2009: Forecasting the solid-to-liquid ratio of precipitation in a cloud-resolving model. Preprints, *23rd Conf. on Weather, Analysis, and Forecasting/19th Conf. on Numerical Weather Prediction*, Omaha, NE, Amer. Meteor. Soc., 7A.2. [Available online at <http://ams.confex.com/ams/pdfpapers/154287.pdf>]
- Noilhan, J., and S. Planton, 1989: A simple parameterization of land surface processes for meteorological models. *Mon. Wea. Rev.*, **117**, 536–549.
- Oberto, E., D. Cane, M. Turco, and P. Bertolotto, 2007: Weather service for the XX Olympic Winter Games: Forecast evaluation. Preprints, *29th Int. Conf. on Alpine Meteorology*, Chambéry, France, WMO.
- Onton, D. J., A. J. Siffert, L. Cheng, W. J. Steenburgh, and B. Haymore, 2001: Regional scale modeling for the 2002 Olympic Winter Games. Preprints, *Ninth Conf. on Mesoscale Processes*, Fort Lauderdale, FL, Amer. Meteor. Soc., J25–J26.
- Stauffer, D. R., G. K. Hunter, A. Deng, J. R. Zielonka, K. Tinklepaugh, P. Hayes, and C. Kiley, 2007: On the role of atmospheric data assimilation and model resolution on model forecast accuracy for the Torino Winter Olympics. Preprints, *22th Conf. on Weather Analysis and Forecasting/18th Conf. on Numerical Weather Prediction*, Park City, UT, Amer. Meteor. Soc., 11A.6. [Available online at <http://ams.confex.com/ams/pdfpapers/124791.pdf>]